An improved MS2 system for accurate reporting of the mRNA life cycle

Evelina Tutucci[1,7], Maria Vera[1,7], Jeetayu Biswas[1], Jennifer Garcia[2], Roy Parker[3,4] & Robert H Singer[1,5,6]

The MS2–MCP system enables researchers to image multiple steps of the mRNA life cycle with high temporal and spatial resolution. However, for short-lived mRNAs, the tight binding of the MS2 coat protein (MCP) to the MS2 binding sites (MBS) protects the RNA from being efficiently degraded, and this confounds the study of mRNA regulation. Here, we describe a reporter system (MBSV6) with reduced affinity for the MCP, which allows mRNA degradation while preserving single-molecule detection determined by single-molecule FISH (smFISH) or live imaging. Constitutive mRNAs (*MDN1* and *DOA1*) and highly-regulated mRNAs (*GAL1* and *ASH1*) endogenously tagged with MBSV6 in *Saccharomyces cerevisiae* degrade normally. As a result, short-lived mRNAs were imaged throughout their complete life cycle. The MBSV6 reporter revealed that, in contrast to previous findings, coordinated recruitment of mRNAs at specialized structures such as P-bodies during stress did not occur, and mRNA degradation was heterogeneously distributed in the cytoplasm.

Imaging single molecules in intact cells reveals the process of gene expression from transcription to translation with high temporal and spatial resolution[1]. One method to visualize single mRNAs in living cells utilizes RNA loops derived from the bacteriophage MS2 coexpressed with its coat protein (MCP)[2]. For mRNA detection, 24 MBS loops are inserted in the 3′ UTR of an mRNA of interest, and coexpression of MCP fused with fluorescent proteins renders single mRNAs visible using wide-field epifluorescence microscopy. This approach has been used in living eukaryotic cells to image single mRNAs from transcription to translation[3–10].

Recent work revealed that MCP binding to MBS impaired mRNA degradation in *S. cerevisiae* and led to the formation of 3′ decay fragments containing MS2 arrays[11–14]. These results called into question whether full-length mRNAs or decay fragments were being observed when an mRNA was tagged using this system. This potential for artifactual results is crucial to understand and alleviate, because the MS2 system has been used to study various aspects of cytoplasmic mRNA regulation[15–17]. To address this problem, the MS2 system was re-engineered so that it mimicked the expression of the endogenous mRNA. The new system can be used to accurately visualize the life cycle of highly regulated mRNA in *S. cerevisiae*, as well as mRNA in mammalian cells.

RESULTS

Characterization of the expression of mRNAs tagged with the MS2–MCP system

The degradation of mRNAs tagged with the MS2–MCP system was characterized using biochemical methods (e.g., northern blot and qPCR)[11,13,14], which did not provide information on the number of cells affected or the amount of degradation in each cell. We used a single-cell approach[12] to measure whether mRNAs tagged with MS2–MCP accumulated 3′ decay fragments in *S. cerevisiae*. Two genes were analyzed: *ASH1*, a cell-cycle-regulated mRNA with a rapid turnover that localizes to the bud tip during anaphase[3,18], and *MDN1*, a constitutively expressed mRNA[19,20]. Both were endogenously tagged with 24xMBS in the 3′ UTR. The latest MBS version, MBSV5, which contains nonrepetitive stem loops arrays[21], was used for *ASH1* (**Fig. 1a**); and MBSORF, with repetitive stem loops without stop codons[20], was used for *MDN1* (**Fig. 1b**). *ASH1* mRNAs endogenously tagged with 24xMBSV5 properly localized to the bud tip during mitosis (**Fig. 1c**). Cells expressed the coat protein fused to two GFP molecules from the constitutive cytochrome C1 promoter (CYC1p), for homogenous expression among cells.

To determine whether each mRNA molecule was intact, the mRNA was probed by two-color smFISH to identify the coding sequence, CDS (*ASH1* or *MDN1*) and the MBS sequence (MBSV5 or MBSORF) (**Fig. 1a–d**). Quantification of *ASH1* mRNAs with FISH-quant[22] using CDS probes showed comparable expression levels whether the mRNA was MS2 tagged, with or without MCP (**Fig. 1e** and **Supplementary Fig. 1a**). Cells expressing MCP had an increased number of MBS molecules without corresponding signal for *ASH1* CDS (3′ decay fragments, **Fig. 1c**,**e**). The number of MBS fragments varied among cells (2.3 times higher than the

[1]Department of Anatomy and Structural Biology, Albert Einstein College of Medicine, Bronx, New York, USA. [2]Department of Molecular Biology, Colorado College, Colorado Springs, Colorado, USA. [3]Department of Chemistry and Biochemistry, University of Colorado Boulder, Boulder, Colorado, USA. [4]Howard Hughes Medical Institute, University of Colorado Boulder, Boulder, Colorado, USA. [5]Gruss-Lipper Biophotonics Center, Albert Einstein College of Medicine, Bronx, New York, USA. [6]Janelia Research Campus of the HHMI, Ashburn, Virginia, USA. [7]These authors contributed equally to this work. Correspondence should be addressed to R.H.S. (robert.singer@einstein.yu.edu).

RECEIVED 29 JUNE; ACCEPTED 4 OCTOBER; PUBLISHED ONLINE 13 OCTOBER 2017; DOI:10.1038/NMETH.4502

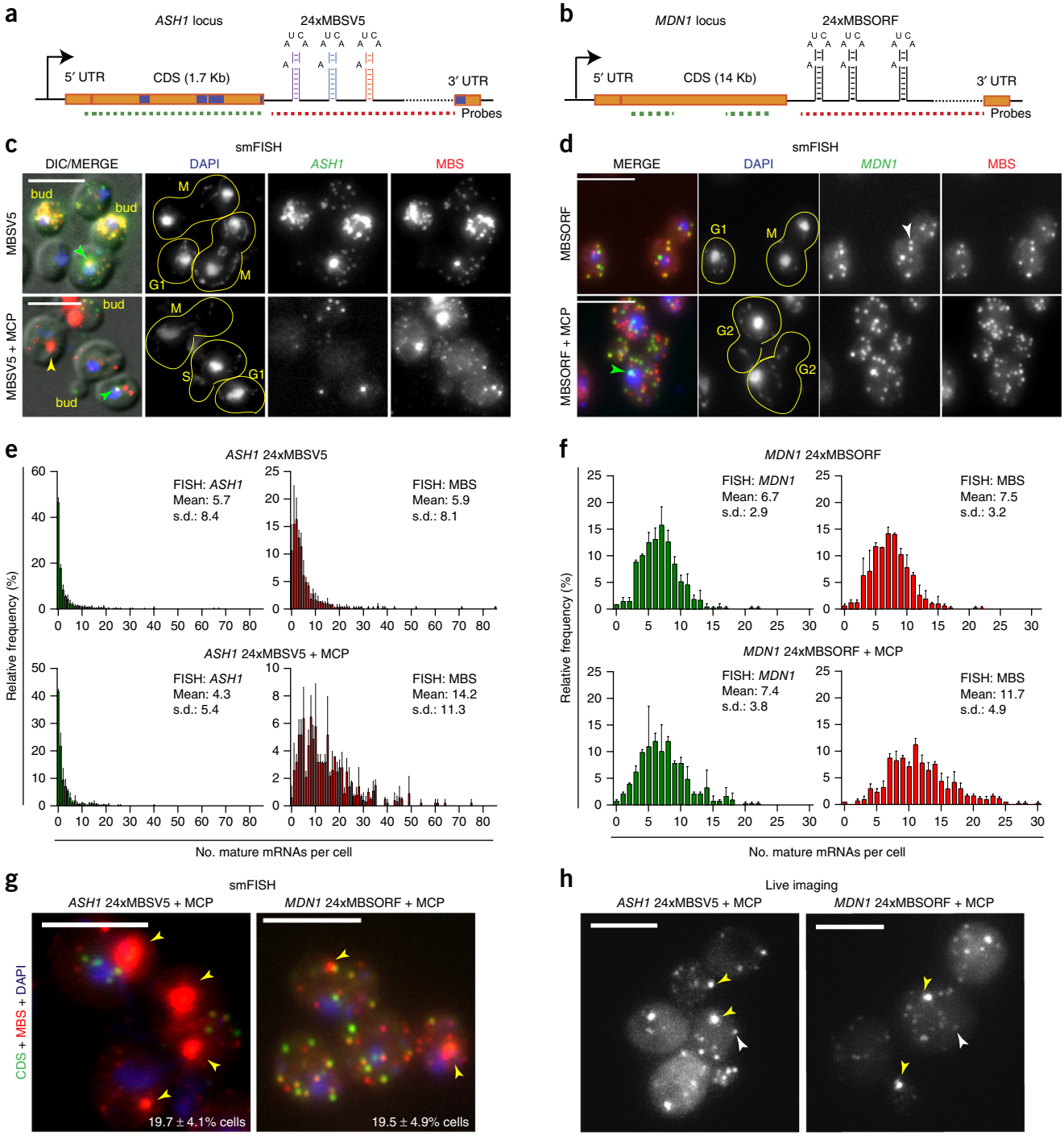

Figure 1 | Previous MBS systems resist degradation in yeast. (**a**,**b**) Scheme of *ASH1* and *MDN1* loci tagged with previously used MBS. (**a**) 24xMBSV5 inserted in the 3′ UTR of endogenous *ASH1* gene. Purple boxes, localization sequences of *ASH1* mRNA. (**b**) 24xMBSORF inserted in the 3′ UTR of the endogenous *MDN1* gene. (**a**,**b**) Dotted lines designate smFISH probe positions recognizing the CDS (green) or MBS sequences (red). (**c**,**d**) Two-color smFISH for (**c**) *ASH1* mRNA tagged with 24xMBSV5 and (**d**) *MDN1* mRNA tagged with 24xMBSORF in cells expressing MCP (YcpLac111 CYC1p-MCP-NLS-2xyeGFP) or the vector alone (YcpLac111). (**c**) DIC/MERGE shows the overlap of the DAPI signal in the nucleus (blue), smFISH for the *ASH1* CDS (green) and the MBS (red) with the differential interference contrast (DIC) image. (**d**) MERGE shows the overlap of the DAPI (blue), smFISH for the *MDN1* CDS (green) and the MBS (red). Yellow lines define the shape of a single cell (the bud position is indicated for the cells expressing *ASH1*). For each cell is indicated the stage of the cell cycle (G1, S, G2 and M phase). White arrowheads, single mRNAs; green arrowheads, transcription sites; yellow arrowheads, MBS aggregates; scale bar, 5 µm. (**e**,**f**) Quantification of smFISH represented in **Figure 1c,d** with CDS probes (green plots) or MBS probes (red plots) reported as frequency distribution of mature (**e**) *ASH1* and (**f**) *MDN1* mRNAs per cell. Mean and s.d. of two independent cell cultures, $n \approx 500$ cells per experiment, and distribution of the mRNAs was generated using the same binning. (**g**) MBS aggregates in the cytoplasm are detected as bright fluorescent spots by smFISH. The percentage indicates cells positive for MBS aggregates. Yellow arrowheads, MBS aggregates. Scale bar, 5 µm. (**h**) MBS aggregates are detected in the cytoplasm of living cells coexpressing MCP. White arrowheads, single *ASH1* (left) and *MDN1* (right) mRNAs; yellow arrowheads, MBS aggregates; scale bar, 5 µm.

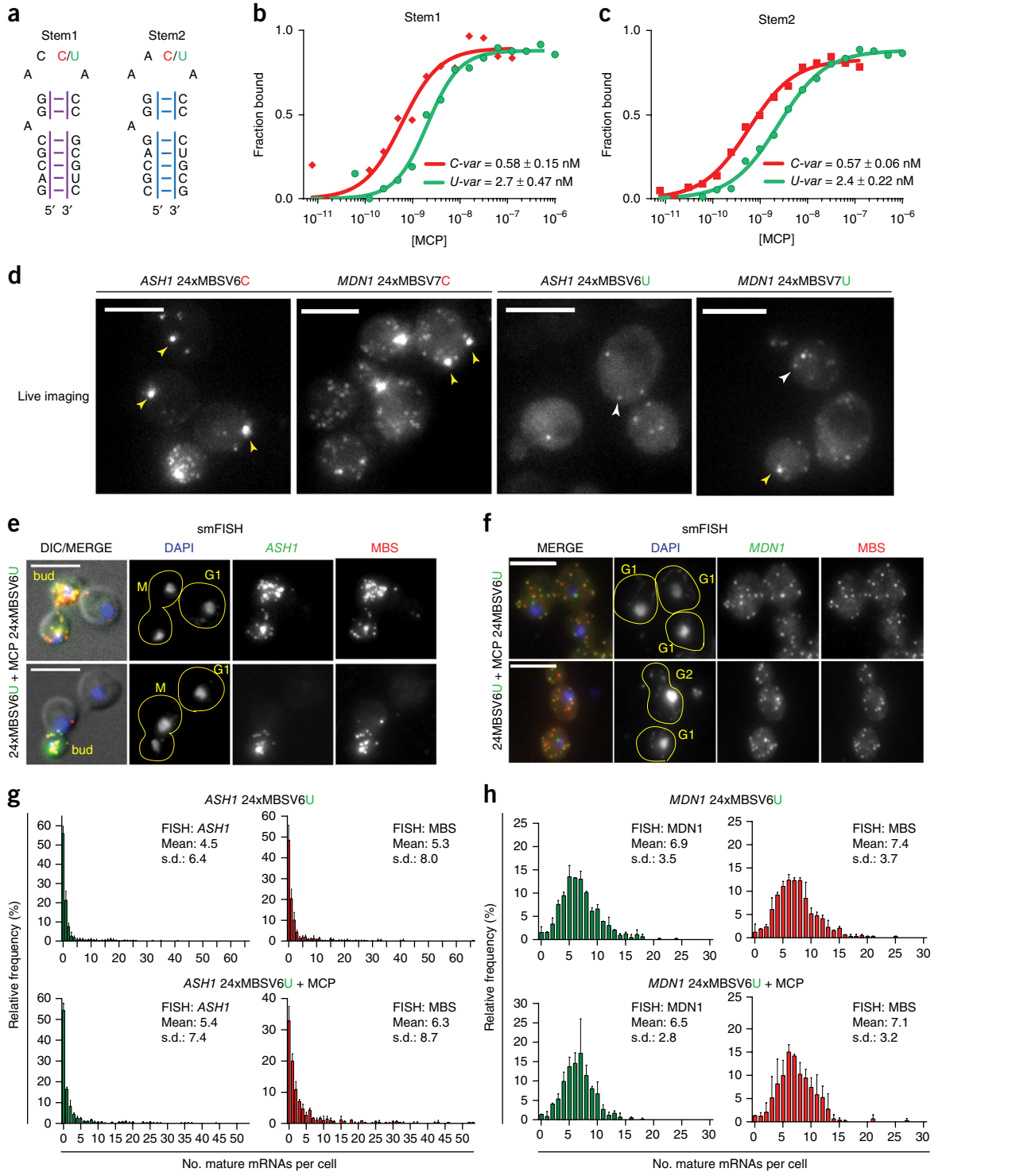

Figure 2 | Design and characterization of a new MS2–MCP system. (**a**) RNA stem loop sequences used for EMSA assays. Stem1 and Stem2 have randomized stem sequence of 7 nt. The two loops were synthesized either as a U variant or C variant at position -5, as indicated. The affinity of MCP for the two stem loops was tested by EMSA. (**b**,**c**) Binding affinity of MCP for the MBS *C-variants* and *U-variants*. The K_d from three independent measurements (**Supplementary Fig. 2f,g**) is indicated on the plots for (**b**) Stem1 and (**c**) the Stem2, either U or C variant. (**d**) Image of living cells coexpressing MCP. (Left) *ASH1* 24xMBSV6 C variant or *MDN1* 24xMBSV7 C variant. (Right) *ASH1* 24xMBSV6 U variant or *MDN1* 24xMBSV7 U variant. Yellow arrowheads, MBS aggregates; white arrowheads, single mRNAs; scale bar, 5 µm. (**e**,**f**) Two-color smFISH for (**e**) *ASH1* mRNAs and (**f**) *MDN1* mRNAs tagged with 24xMBSV6 in cells expressing MCP or the vector alone. (**e**) DIC/MERGE shows the overlap of the DAPI (blue), smFISH for the *ASH1* CDS (green) and the MBSV6 (red) with the DIC image. (**f**) MERGE shows the overlap of the DAPI signal (blue), smFISH for the *MDN1* CDS (green) and the MBSV6 (red). Yellow lines define the shape of a single cell. For each cell is indicated the cell cycle stage. Scale bar, 5 µm. (**g**,**h**) Quantification of smFISH represented in **Figure 2e,f** with CDS probes (green plots) or MBS probes (red plots) reported as frequency distribution of mature (**g**) *ASH1* and (**h**) *MDN1* mRNAs per cell. Mean and s.d. of two independent cell cultures, $n \approx 500$ cells per experiment.

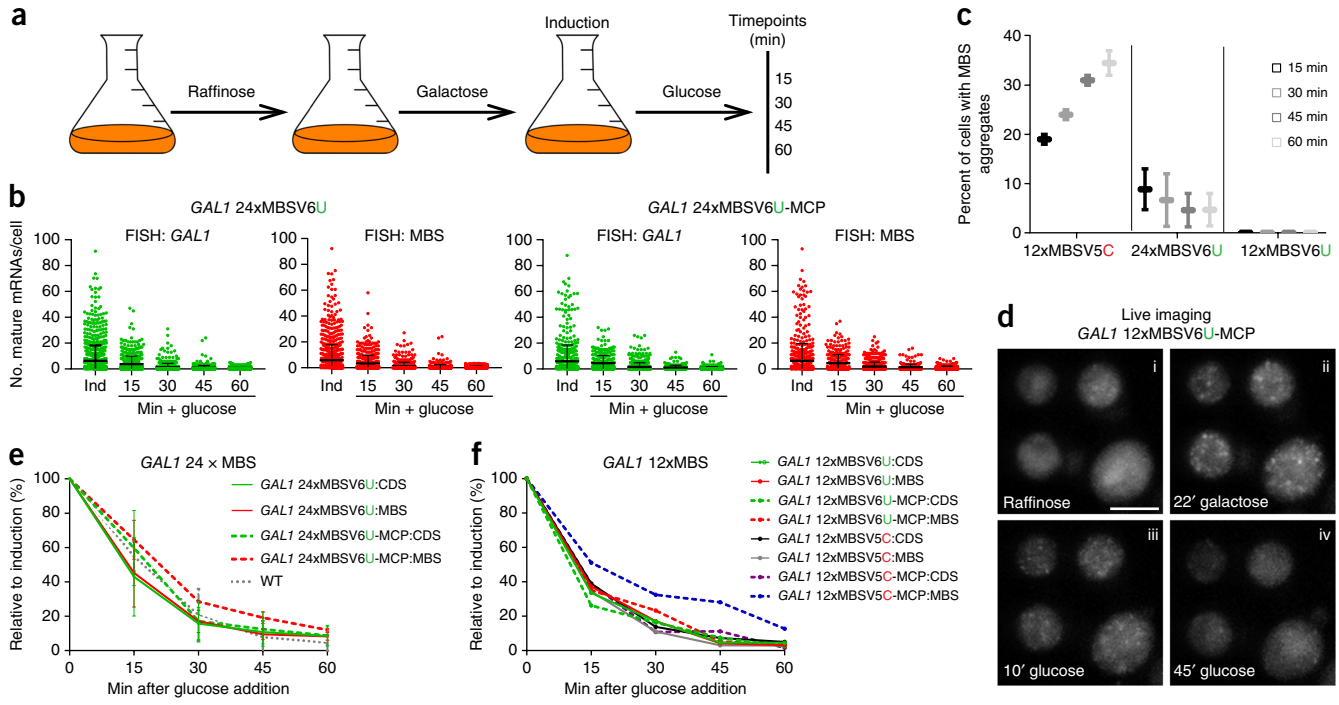

Figure 3 | 12xMBSV6 faithfully reports the rapid degradation of *GAL1* mRNA. (**a**) Scheme of protocol used to control *GAL1* mRNA expression. (**b**) Quantification of smFISH for *GAL1* 24xMBSV6 mRNAs in cells expressing: left, vector alone or right: MCP. Each dot represents the quantification obtained from a single cell with probes binding the CDS (green) or the MBSV6 (red). Error bars indicate the mean and s.d. from three independent cell cultures. (**c**) Percentage of cells with MBS aggregates derived from the degradation of *GAL1* mRNA tagged with the current and new MBS systems at different times after glucose addition. Mean and s.d. from two independent cell cultures. MBS aggregates were not detected for cells coexpressing *GAL1* 12xMBSV6 and MCP. (**d**) Representative images of **Supplementary Video 1** of *GAL1* 12xMBSV6–MCP. Time indicates the minutes cells were shifted from raffinose (i) to galactose (ii) and then to glucose (iii,iv). (**e**) Plots of *GAL1* mRNA decay obtained from the quantification described in **Figure 2b**. The mean number of mRNAs at each timepoint was normalized to the induced condition (100%) and reported as a percentage. WT indicates the quantifications of smFISH performed with *GAL1* CDS probes on an untagged (wt) strain. Nonsignificant differences between the half-life measured with the CDS or MBS probes (paired *t*-test, *P* values are reported in **Supplementary Table 2**). Mean and s.d. are calculated from three independent cultures. (**f**) Plots of *GAL1* mRNA decay tagged with 12xMBSV5 or V6. The mean number of mRNAs at each timepoint was normalized to the induced condition (100%) and reported as a percentage. The plots represent one experiment from two independent cell cultures.

full-length *ASH1* mRNA), and this provided an erroneous frequency distribution (**Fig. 1e**) similar to that of *MDN1* mRNAs tagged with 24xMBSORF (**Fig. 1d**,**f**). The expression of endogenous *MDN1* was constitutive (a Gaussian distribution that ranges from 0 to ~15 mRNAs per cell[19]; **Supplementary Fig. 1b**). The number of MBS spots doubled in the presence of the MCP relative to the mRNAs quantified with the CDS probes (**Fig. 1f**). In about 20% of cells coexpressing MCP and tagged with *ASH1* or *MDN1*, bright aggregates were seen. These aggregates, which contained only the MBS sequence, resulted from the accumulation of single MBS fragments bound by MCP and were present even when the number of MBSV5 stem loops was reduced to 12 (**Fig. 1g**, **Supplementary Fig. 1c**,**d** and **Supplementary Note 1**).

The results of live imaging were consistent with the smFISH results. Live imaging of strains expressing MCP with tagged *ASH1* or *MDN1* revealed that 20% of the cells contained one to two MBS aggregates per cell that were less mobile and brighter than single molecules (**Fig. 1h** and **Supplementary Table 1**). These aggregates were absent in cells that expressed MCP alone, which indicated that the formation of aggregates required both MBS and MCP (**Supplementary Fig. 1e**). The binding of the MCP to the MBS allowed proper expression and localization of *ASH1* mRNA at the bud tip but delayed degradation of the MBS, which accumulated as aggregates (see **Supplementary Fig. 1f** and **Supplementary Note 2** regarding previous *ASH1* publications[3]). Accumulation of MBS fragments was accentuated for highly regulated and short-lived mRNAs, like *ASH1*, more than for constitutively expressed and stable mRNAs like *MDN1*, since fewer molecules at any one time are degrading. Hence, the use of the available MS2–MCP systems in living yeast can lead to incorrect conclusions about mRNA expression and localization. Consequently, mRNA tagging must be validated by two-color smFISH or by other approaches.

Design of a degradable MS2–MCP system faithfully recapitulating mRNA kinetics

Early work on the wild-type bacteriophage MS2 identified a uridine at position -5 (U variant) of the loop (**Supplementary Fig. 2a**) that, when substituted by a cytosine (C variant), increased the affinity of the MCP 10-fold (K_d from 10 nM to 1 nM) and decreased the dissociation kinetics about 90-fold[23,24]. We reproduced these results with the MCP used for imaging by electrophoretic mobility shift assay (EMSA) (**Supplementary Fig. 2d**–**f**). Because the higher affinity of the C variant would retain the tag on the mRNA longer, it was originally used to image single mRNA molecules in living eukaryotic cells[3,4]. Because the current MBSV5 and MBSORF versions contain the C-variant[20,21] (**Supplementary Fig. 2b**,**c**), we posited that the lower affinity U-variant would facilitate degradation.

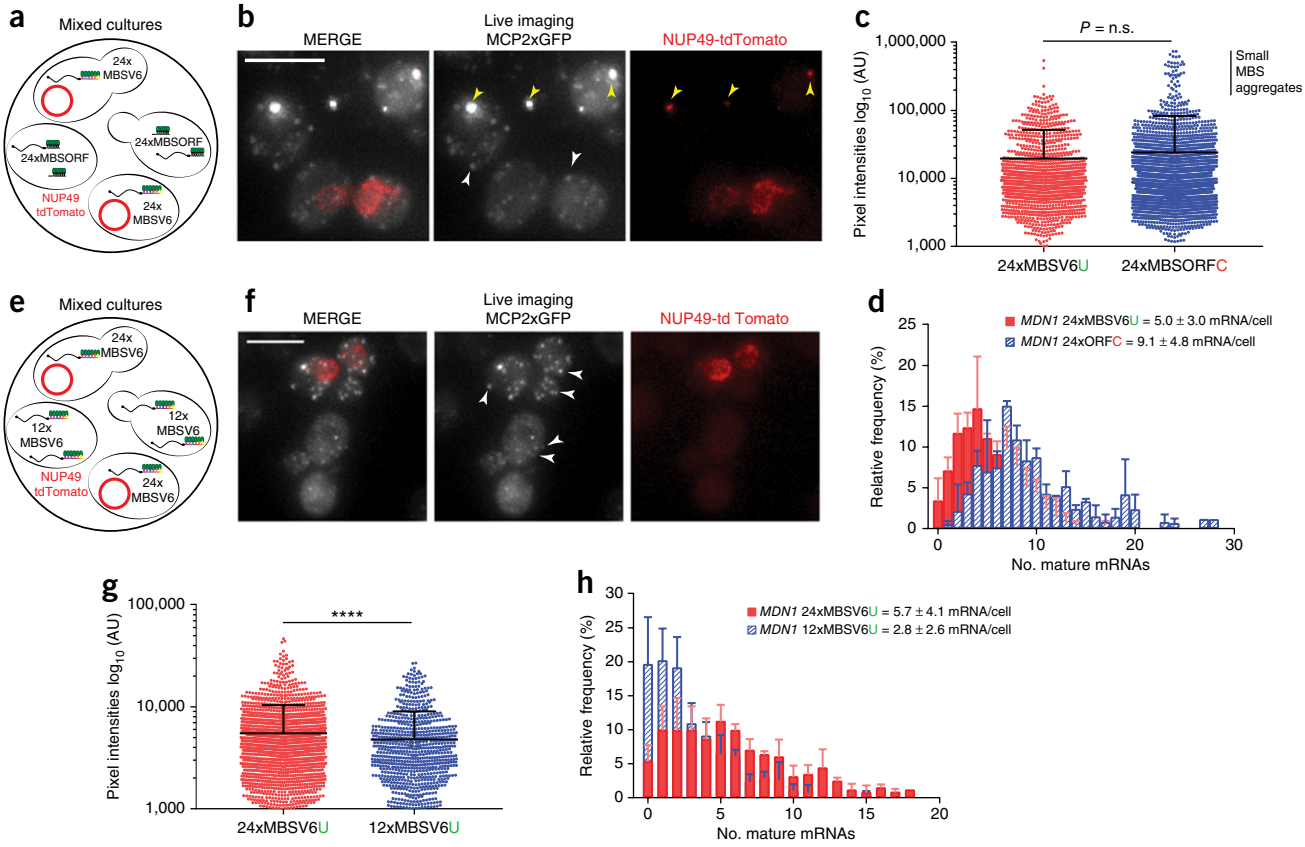

Figure 4 | MBSV6–MCP maintains single-mRNA resolution in living cells. (**a**) Scheme of the mixed cultures used to compare the intensity of single *MDN1* mRNAs tagged with either 24xMBSV6 or 24xMBSORF. Cells expressing 24xMBSV6 or 24xMBSV6. Cells expressing 24xMBSV6–MCP coexpress Nup49–tdTomato marking the nuclear envelope (red circle). (**b**) Two-color live imaging of the mixed cultures. MERGE shows the mRNA signal (gray) and Nup49tdTomato (red). Yellow arrowheads, MBS aggregates containing GFP that 'bleedthrough' the red channel; white arrowheads, single mRNAs. (**c**) Plot of the intensities of single *MDN1* mRNAs tagged with either 24xMBSV6 (n = 1,246) or 24xMBSORF (n = 2,271). Cells with large aggregates visible in the red channel were excluded. Nonparametric Mann-Whitney test does not show significant difference in brightness, P = 0.6753. AU, arbitrary units. (**d**) Frequency distribution of *MDN1* from sample in **b** and **c**. (**e**) Scheme of the mixed cultures to compare the intensity of single *MDN1* mRNAs tagged with either 24xMBSV6 or 12xMBSV6. Cells expressing 24xMBSV6–MCP coexpress Nup49–tdTomato (red circle). (**f**) Two-color live imaging of the mixed cultures. MERGE shows the mRNA signal (gray) and Nup49tdTomato (red). White arrowheads, single mRNAs. (**g**) Plot of the intensities of single *MDN1* mRNAs tagged with either 24xMBSV6 (n = 1,684) or 12xMBSV6 (n = 861). Nonparametric Mann–Whitney test shows significant difference in brightness, P < 0.0001. (**h**) Frequency distribution of *MDN1* mRNAs from sample in panels **f** and **g**. For all experiments, error bars represent the mean and s.d. of three independent cultures; n = 100 cells per experiment.

Since the MBS–MCP complex inhibited degradation of the stem loops, we tested the effect of both the stems and the loops independently by EMSA. The current MS2 arrays contain synonymized loop sequences to avoid recombination. We tested whether changing the stem sequence affected the affinity for MCP. We compared two different stems of 7 bp (Stem1 and Stem2), each with a U or C variant in the loop (**Fig. 2a**). Apparent equilibrium dissociation constants (K_d) were extracted from plots of MCP bound versus free (**Fig. 2b**,**c** and **Supplementary Figs. 2g**,**h**). For Stem1 and Stem2, the C to U mutation was sufficient to reduce ten times the affinity of the CP for the MBS independently of the stem sequence (**Fig. 2b**,**c**). Two other strategies were attempted to increase the degradation of the MBS–MCP arrays in living cells. The lengths of the linkers were increased from 30 nt to 50 (MBSV6) or 40 nt (MBSV7), which would possibly allow better access of nucleases to the mRNA, and the stem loops were reduced to 12 from 24, which provided less substrate for degradation (**Supplementary Fig. 3a**–**c**).

Live imaging of cells expressing MCP with C variants of either *ASH1* 24xMBSV6 or *MDN1* 24xMBSV7 revealed MBS aggregates in the cytoplasm (**Fig. 2d**, left). Hence, increasing the length of the linkers did not prevent the formation of large MBS aggregates. In contrast, these large MBS aggregates, as defined by a spectral overlap ('bleedthrough') criterion, were not observed in cells with the lower affinity U variants (**Fig. 2d**, right). Importantly, single mRNA molecules could be detected in cells. However, since the detection during live imaging is only by the MBS–MCP, it was not clear that the full mRNAs were observed.

smFISH of endogenous mRNAs tagged with U variants MBSV6 and MBSV7

To determine whether the tagged mRNAs were full length, or if they accumulated as MBS fragments, U-variants of MBSV6 or MBSV7 were tested by two-color smFISH. Characterization of the expression of mRNAs tagged with MBSV7 still showed cells with fragments and small MBS aggregates (**Supplementary Fig. 3d**,**e** and **Supplementary Note 3**). In contrast, cells expressing 24xMBSV6, avoided the formation of MBS–MCP aggregates and had few fragments. Moreover, the distributions and the mean of mRNAs, whether using probes to the CDS or MBS, were similar (**Fig. 2e**–**h**), as was revealed by the correlation analysis (**Supplementary**

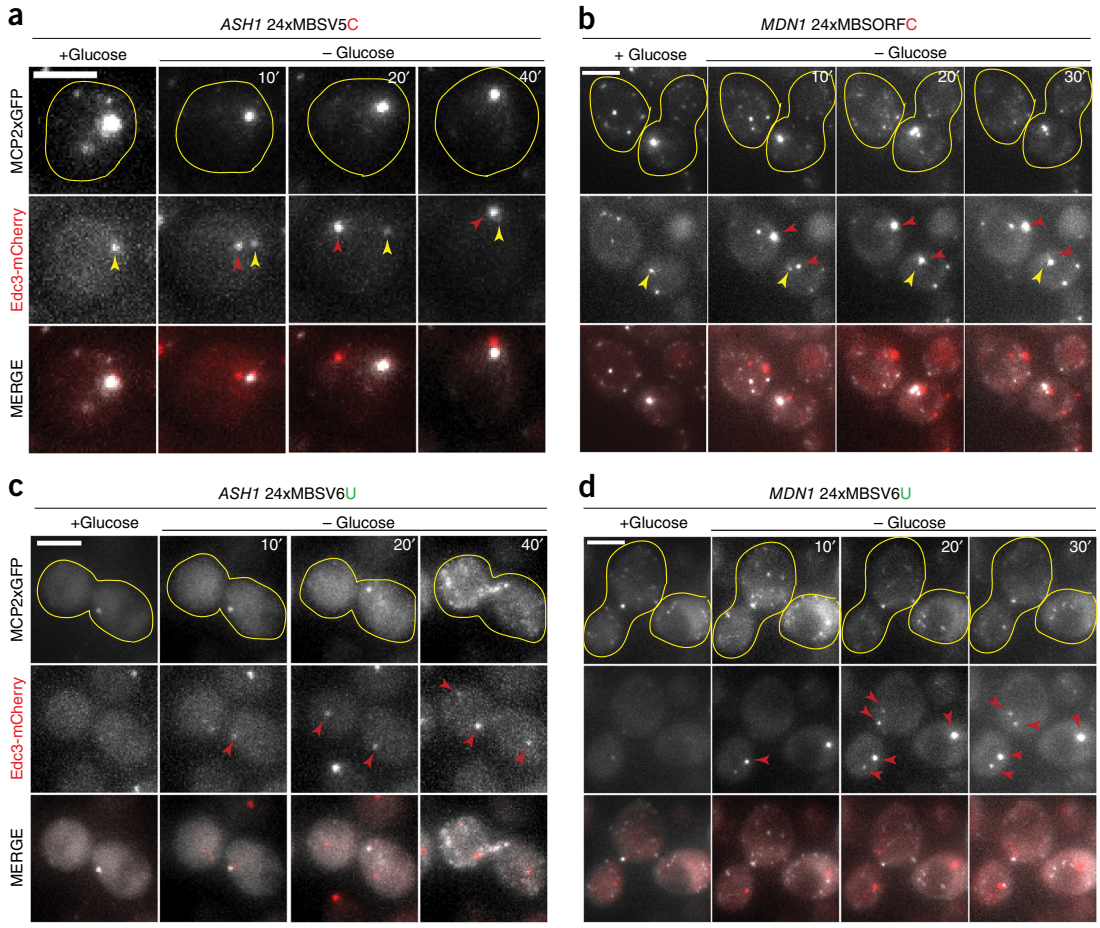

Figure 5 | MBSV6–MCP enables single-mRNA imaging under stress conditions. (**a**–**d**) Live imaging of mRNAs tagged with 24xMBS–MCP in cells expressing the PB marker Edc3–mCherry. (**a**,**c**) *ASH1* mRNAs tagged with either 24xMBSV5–MCP or 24xMBSV6–MCP. (**b**,**d**) *MDN1* mRNAs tagged with either 24xMBSORF–MCP or 24xMBSV6–MCP. MERGE indicates the overlap between the mRNA signal (gray) and Edc3–mCherry signal (red). Yellow lines define the shape of a single cell. Yellow arrowheads, 'bleedthrough' from MBS aggregates; red arrowheads, PBs. Representative images from **Supplementary Videos 2** and **3**. Time after glucose starvation (left to right, intervals in min). Scale bar, 3 μm.

Fig. 3f,**g**). Reducing the number of stem loops from 24 to 12 further increased the degradation of MBSV6 (**Supplementary Fig. 4a**,**b**). Quantification with either MBS or CDS probes in cells expressing MCP gave the same results (nonparametric *t*-test, Mann–Whitney test) (**Supplementary Fig. 4c**–**e**).

To confirm that mRNAs tagged with the new MSB–MCP systems were full length, northern blot analysis was performed using a probe hybridizing to the *ASH1* mRNA after the site of MBS integration (**Supplementary Fig. 5a**,**b**). Consistent with previous observations[11,13,14], *ASH1* mRNAs tagged with C-variant 24xMBSV5 and coexpressed with MCP showed the accumulation of MBS fragments (**Supplementary Fig. 5a**,**b**). In contrast, *ASH1* mRNAs tagged with U variants MBSV7 and MBSV6, either 24 or 12 MBS showed reduced accumulation of MBS fragments, consistent with the results observed by smFISH. The MBSV6 gave fewer decay products as compared to the MBSV5 version for the highly expressed *GAL1* gene as well, which indicated that the MBSV6 version greatly reduced mRNA decay fragments with diverse mRNAs (**Supplementary Fig. 5c**). Therefore, tagging of *ASH1*, *MDN1* or *GAL1* genes with the MBSV6 system recapitulated the endogenous pattern of expression and the expected cellular localization of the full-length mRNA, even when bound by MCP.

MBSV6 reports rapid changes in mRNA degradation

The rapid kinetics of *GAL1* mRNA in yeast provided a means to determine whether MBSV6 degrades simultaneously with the CDS and accurately reports on mRNA decay. *GAL1* responds to rapid changes in carbon source[25]. Shifting cells from glucose to raffinose generates a preinduced state, which leads to a rapid induction of *GAL1* upon galactose addition. Conversely, washing out galactose and adding glucose inhibits *GAL1* transcription and induces *GAL1* mRNA decay[26], and this allows comparison of *GAL1* CDS half-life ($t_{1/2}$) with MBS $t_{1/2}$ when protected or unprotected by MCP (**Fig. 3a**).

The degradation of MBSV6–MCP compared with that of MBSV5–MCP was analyzed by two-color smFISH in yeast strains expressing the *GAL1* mRNA tagged with 12xMBSV6, 24xMBSV6 or 12xMBSV5, with and without MCP (**Supplementary Fig. 6a**). Cells growing in raffinose did not express *GAL1* mRNA (**Supplementary Fig. 6a**, Ctrl). Addition of 0.2% galactose for 30 min triggered the induction of *GAL1* mRNA expression (**Fig. 3b** and **Supplementary Fig. 6b**,**c**). After switching to glucose, the number of single molecules detected by probes to CDS or MBS declined over time in the presence or absence of MCP and reached undetectable levels after 60 min (**Fig. 3b** and

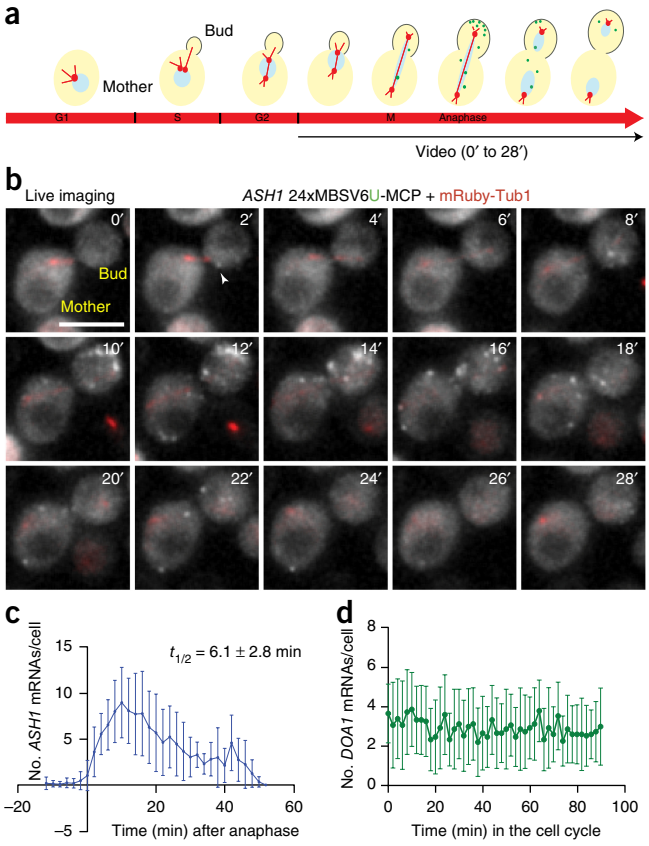

Figure 6 | MBSV6–MCP quantitatively reports *ASH1* mRNA levels throughout the cell cycle. (**a**) Scheme of *ASH1* mRNA expression during the cell cycle (marked on red arrowhead). Green dots represent *ASH1* mRNA. mRubyTub1 (red) marks the spindle pole body, duplicated during S phase. The bud emergence (outlined) starts during S-phase and ends with the formation of the daughter cell. The black arrow indicates the corresponding cell cycle phase of the video in **Figure 6b**. (**b**) Representative images of **Supplementary Video 4**. Simultaneous two-color imaging of cells coexpressing *ASH1* 24xMBSV6-MCP (gray) and mRubyTub1 (red). Time 0 indicates the beginning of anaphase. Images were acquired every 2 min. White arrowhead, single mRNAs. Scale bar, 5 µm. (**c**) Quantification of single *ASH1* mRNAs during the cell cycle. Time 0 indicates the beginning of anaphase (n = 21). During mitosis, *ASH1* decayed with a $t_{1/2}$ of 6.1 ± 2.8 min. (**d**) Quantification of single *DOA1* mRNAs tagged with 24xMBSV6–MCP during the complete cell cycle (n = 15). Images were acquired every 2 min (**Supplementary Video 4**).

Supplementary Fig. 6a–c). Cells expressing 12xMBSV5–MCP increased the formation of large MBS aggregates over time after glucose supplementation (**Fig. 3c** and **Supplementary Fig. 6d**). However, fewer than 10% of cells tagged with 24xMBSV6-MCP showed smaller MBS aggregates (**Fig. 3c**, **Supplementary Fig. 6a** and **Supplementary Video 1**). The number of MBS molecules per aggregate and the percentage of cells with aggregates decreased over time for the *GAL1* tagged with 24xMBSV6 (**Fig. 3c** and **Supplementary Fig. 6e**). MBS aggregates were not observed in 12xMBSV6 (**Fig. 3c**). The decay of *GAL1* 12xMBSV6–MCP induced by glucose was observed over the course of 1 h by live imaging (**Fig. 3d** and **Supplementary Video 1**).

Tagging of *GAL1* with 24xMBSV6 shortened its half-life to $t_{1/2}$ = 11 min, possibly on because of a change in length or sequence of 3′ UTR (**Fig. 3e**, **Supplementary Table 2** and **Supplementary Note 4**). The curves obtained for the CDS and the MBS probes were practically identical (**Fig. 3e**). Furthermore, in the presence of MCP, the $t_{1/2}$ obtained with the MBS probes (**Fig. 3e**), although slightly longer, was not significantly different (paired t-test) than the one obtained with the CDS probes or the endogenous *GAL1* (**Fig. 3e** and **Supplementary Table 2**). In cells expressing *GAL1* 12xMBSV6–MCP, the CDS and the MBS sequences were degraded simultaneously, in contrast to 12xMBSV5 (**Fig. 3f** and **Supplementary Table 2**). Therefore, in the case of highly inducible genes where the mRNAs were degraded in a short period of time, reducing the number of MBSV6 repeats from 24 to 12 prevented the formation of MBS aggregates and enabled precise measurement of their abundance and degradation rate.

Characterization by live imaging of mRNAs tagged with MBSV6

Since MBSV6 was an accurate reporter of mRNA decay by smFISH, we tested whether it could be reliably used in living cells. The brightness of constitutively expressed single *MDN1* mRNAs tagged with 24xMBSORF or 24xMBSV6 MCP systems was compared. Mixed cultures were differentiated by the expression of the nuclear pore protein Nup49 tagged with tdTomato only in the strain expressing MBSV6 (**Fig. 4a**,**b**). The average intensity of single *MDN1* mRNAs was determined for each strain, and significant differences were not found (P = 0.675; **Fig. 4c**). The cytoplasmic MBS aggregates in the 24xMBSORF–MCP-expressing cells were excluded from the analysis because they crossed into the red channel (**Fig. 4b**, yellow arrowheads). The average number of mRNAs counted in cells expressing *MDN1*–24MBSV6 or *MDN1*–24MBSORF closely resembled the number counted with smFISH (**Fig. 4d** compared with **Fig. 1f** and **2h**). Thus, the detection of single molecules was not affected by the reduction of affinity of MCP for the MBSV6 U variant. MBSV6 was also used to visualize single mRNAs in mammalian cells, as with the previously characterized MBSV5 system[6,21], without significant loss of brightness (**Supplementary Fig. 7a**,**b** and **Supplementary Note 5**).

To define the optimal number of loops required to detect single mRNAs, we compared the brightness of *MDN1* mRNAs tagged either with 12x MBSV6 or 24xMBSV6 under the same imaging conditions (**Fig. 4e–g**). Mixed cultures, differentiated by Nup49–tdTomato in the strain expressing 24xMBSV6, showed that *MDN1* mRNAs tagged with 12xMBSV6 were, on average, 15% dimmer than the ones tagged with 24xMBSV6 (**Fig. 4e–g**; nonparametric Mann–Whitney test, P < 0.0001). A similar loss of intensity from the MBS signal was quantified by smFISH (**Supplementary Fig. 7c**). However, the decrease in brightness of *MDN1* 12xMBSV6 compared to that of 24xMBSV6 reduced the number of detected single molecules by 50%, while no reduction was observed by smFISH (**Fig. 4h** and **Supplementary Fig. 7d**). In the case of *MDN1*, the 12xMBSV6–MCP system detected 65 to 75% of the mRNA molecules that were detected by smFISH. These results suggest that 24xMBSV6 better reported individual mRNAs in living cells.

mRNA localization during stress induced by glucose starvation

The MS2–MCP system has been used to colocalize mRNAs with processing bodies (PBs), stress granules or peroxisomes during stress conditions[15,16,27,28]. However, a recent report suggested that

only the MBS fragments, but not the CDS of the tagged mRNA, colocalize with PBs[12]. To ensure that the MBSV6 system faithfully reported mRNA localization during stress, we used live imaging to visualize *ASH1* or *MDN1* mRNAs and PB markers during glucose starvation. We monitored PB formation by coexpressing the decapping cofactor Edc3 fused to mCherry[29,30] in cells where *ASH1* or *MDN1* was tagged with either the previous 24xMS2–MCP systems or 24xMBSV6–MCP. Cells expressing *ASH1* or *MDN1* tagged with the previous systems showed cytoplasmic MBS aggregates even before glucose deprivation in both channels and substantial 'bleedthrough' that could affect interpretation of colocalization with a second labeled component (**Fig. 5a**,**b**, yellow arrowheads; **Supplementary Fig. 8c**,**d**; **Supplementary Videos 2** and **3**; and **Supplementary Note 6**). In contrast, cells expressing *ASH1* and *MDN1* mRNAs tagged with 24xMBSV6–MCP did not form MCP aggregates during glucose starvation and did not recruit single *ASH1* and *MDN1* mRNAs, which are not required for the stress response, to PBs (**Fig. 5c**,**d** and **Supplementary Videos 2** and **3**). smFISH was used to confirm the integrity of the *ASH1* and *MDN1* mRNAs and the induction of the stress response (*HSP104*) (**Supplementary Fig. 8a**,**b** and **Supplementary Note 6**). These results validated the use of the MBSV6–MCP system for analyzing mRNA localization and decay during stress conditions.

Expression of *ASH1* mRNA during the cell cycle

Cell-cycle-regulated genes are characterized by precise control of their synthesis and degradation[31]. In yeast, *ASH1* mRNA expression is temporally restricted to anaphase, and the mRNA localizes to the bud tip, where it is locally translated to control mating-type switching[18,32,33]. To quantify *ASH1* mRNAs during the cell cycle, *ASH1* was tagged with 24xMBSV6, and cell-cycle progression was monitored with the *TUB1* gene tagged with mRuby (**Fig. 6a**). The microtubules extend from the spindle pole body between the mother and daughter cell, participating in chromosome separation and mitosis[34] (**Fig. 6a**). *ASH1* mRNA expression was preceded by microtubule stretching, which allowed the clear identification of mother–daughter pairs and cell-cycle phase (**Fig. 6a**,**b**). The number of single *ASH1* mRNAs for each timepoint was counted (a representative cell is shown and quantified in **Fig. 6b**, **Supplementary Fig. 9a** and **Supplementary Video 4**). The quantification of 21 cells showed that *ASH1* mRNA was expressed during 30 min corresponding to anaphase (**Fig. 6c**). We measured a $t_{1/2}$ (5.6–6.1 min) consistent with recent reports that the full cycle of *ASH1* mRNA lasted about 30 min, and the mean $t_{1/2}$ was 6.3 ± 1 min (**Fig. 6c** and **Supplementary Fig. 9a**)[35]. We observed bursts of transcription in the mother followed by localization of mRNAs to the bud tip; before the end of mitosis, a second burst of accumulation occurred in the bud tip from transcription in the daughter (**Supplementary Fig. 9b**, **Supplementary Video 5** and **Supplementary Note 7**). The *ASH1* mRNAs in the daughter cell stayed for a prolonged period before degradation.

To demonstrate that the disappearance of the mRNA signal is caused by mRNA decay and not fading of the MCP–GFP signal during the time of observation, we used same imaging conditions to follow the *DOA1* gene, which was constitutively expressed throughout the cell cycle[31] (**Supplementary Fig. 9c**–**e**). The number of single *DOA1* molecules quantified over the cell cycle was constant, with an average of 2.9 ± 1.1 mRNAs per cell (**Fig. 6d** and **Supplementary Video 4**), which was consistent with two-color smFISH experiments (**Supplementary Fig. 9e**). These experiments demonstrated that the MBSV6 system provided the temporal and spatial resolution required to quantify the expression of mRNAs from birth to death in living cells.

DISCUSSION

The MS2–MCP system has been extensively used to study the regulation of gene expression by following endogenously tagged mRNAs[1]. The use of C variant MBS is appropriate for mammalian cells where mRNAs with long half-lives are investigated[36] (**Supplementary Table 1**). However, in yeast where the mRNA half-life is short, and degradation of the MBS becomes rate limiting, the MBS can accumulate as individual fragments or aggregates[11–14]. Other systems to detect endogenous mRNA molecules, such as the Spinach or MANGO aptamers[37,38] or the RCas9 system[39], require additional evaluation of target specificity, formation of artifacts and reliability on reporting single mRNAs. Therefore, we engineered and characterized a new MS2–MCP system that prevented the formation of MBS aggregates by reducing the binding affinity between the MBS and MCP (**Supplementary Note 8**). MBSV6 faithfully recapitulated the life cycle of the mRNA while preserving single-molecule resolution.

Previous reports using MBS C-variant systems suggested that during stress, mRNAs not involved in the stress response (such as *MDN1* or *ASH1*), accumulate in cytoplasmic structures such as PBs, where the mRNAs are stored or degraded[15,40]. Coordinated recruitment of *MDN1* or *ASH1* mRNAs tagged with MBSV6 to PBs was not observed, which suggested that the role of PBs as mRNA storage sites during stress should be re-evaluated. To characterize the role of PBs and other cytoplasmic structures in coordinating the cellular response to stress, the MBSV6–MCP offers the spatial and temporal resolution to elucidate the interactions of mRNAs and RNA-binding proteins, when they form cytoplasmic mRNP granules. These two-color experiments would also provide insights on mRNA decay and on the kinetics of assembly and disassembly of stress granules. The approach can be also used to validate mRNAs tagged with orthologous systems, such as PP7[41], lambda boxB RNA[42] or U1A[43].

The modified MS2 system provides a new capability for imaging and measuring the regulatory events of the entire RNA lifetime without perturbation (**Supplementary Fig. 10** and **Supplementary Tables 1** and **3**). In particular, the decay events of single RNAs in single cells can now be elucidated with temporal and spatial resolution sufficient to study the localization and function of highly unstable RNAs, such as noncoding or regulatory RNAs, as well as the binding proteins regulating them.

METHODS

Methods, including statements of data availability and any associated accession codes and references, are available in the online version of the paper.

Note: Any Supplementary Information and Source Data files are available in the online version of the paper.

ACKNOWLEDGMENTS

We thank X. Meng for help with cloning; D. Muhlrad for help with the northern blots; B. Wu for writing the script to generate the new MBS system; and C. Eliscovich, Y. Yoon and S. Das for critical reading. This work was supported by NIH grant GM57071 to R.H.S. R.P. was supported by HHMI. E.T. was supported

by Swiss National Science Foundation Fellowships P2GEP3_155692 and P300PA_164717. J.B. was supported by training support for AECOM (T32GM007288) and a predoctoral NIH fellowship (F30CA214009). J.G. was supported by NIH grant F32 GM10807.

AUTHOR CONTRIBUTIONS

E.T. and M.V. designed and performed the experiments and analyzed the data. J.B. performed EMSAs. J.G. performed the northern blot. E.T., M.V. and R.H.S. conceived ideas and wrote the manuscript with input from R.P. R.H.S. supervised the research.

COMPETING FINANCIAL INTERESTS

The authors declare competing financial interests: details are available in the online version of the paper.

1. Vera, M., Biswas, J., Senecal, A., Singer, R.H. & Park, H.Y. Single-cell and single-molecule analysis of gene expression regulation. *Annu. Rev. Genet.* **50**, 267–291 (2016).
2. Bernardi, A. & Spahr, P.F. Nucleotide sequence at the binding site for coat protein on RNA of bacteriophage R17. *Proc. Natl. Acad. Sci. USA* **69**, 3033–3037 (1972).
3. Bertrand, E. *et al.* Localization of *ASH1* mRNA particles in living yeast. *Mol. Cell* **2**, 437–445 (1998).
4. Grünwald, D. & Singer, R.H. *In vivo* imaging of labelled endogenous β-actin mRNA during nucleocytoplasmic transport. *Nature* **467**, 604–607 (2010).
5. Larson, D.R., Zenklusen, D., Wu, B., Chao, J.A. & Singer, R.H. Real-time observation of transcription initiation and elongation on an endogenous yeast gene. *Science* **332**, 475–478 (2011).
6. Wu, B., Eliscovich, C., Yoon, Y.J. & Singer, R.H. Translation dynamics of single mRNAs in live cells and neurons. *Science* **352**, 1430–1435 (2016).
7. Halstead, J.M. *et al.* Translation. An RNA biosensor for imaging the first round of translation from single cells to living animals. *Science* **347**, 1367–1671 (2015).
8. Morisaki, T. *et al.* Real-time quantification of single RNA translation dynamics in living cells. *Science* **352**, 1425–1429 (2016).
9. Lim, B., Levine, M. & Yamazaki, Y. Transcriptional pre-patterning of *Drosophila* gastrulation. *Curr. Biol.* **27**, 286–290 (2017).
10. Tantale, K. *et al.* A single-molecule view of transcription reveals convoys of RNA polymerases and multi-scale bursting. *Nat. Commun.* **7**, 12248 (2016).
11. Garcia, J.F. & Parker, R. MS2 coat protein bound to yeast mRNAs block 5′ to 3′ degradation and trap mRNA decay products: implications for the localization of mRNAs by MS2-MCP system. *RNA* **21**, 1393–1395 (2015).
12. Heinrich, S., Sidler, C.L., Azzalin, C.M. & Weis, K. Stem–loop RNA labeling can affect nuclear and cytoplasmic mRNA processing. *RNA* **23**, 134–141 (2017).
13. Garcia, J.F. & Parker, R. Ubiquitous accumulation of 3′ mRNA decay fragments in *Saccharomyces cerevisiae* mRNAs with chromosomally integrated MS2 arrays. *RNA* **22**, 657–659 (2016).
14. Haimovich, G. *et al.* Use of the MS2 aptamer and coat protein for RNA localization in yeast: a response to "MS2 coat proteins bound to yeast mRNAs block 5′ to 3′ degradation and trap mRNA decay products: implications for the localization of mRNAs by MS2-MCP system". *RNA* **22**, 660–666 (2016).
15. Sheth, U. & Parker, R. Decapping and decay of messenger RNA occur in cytoplasmic processing bodies. *Science* **300**, 805–808 (2003).
16. Zid, B.M. & O'Shea, E.K. Promoter sequences direct cytoplasmic localization and translation of mRNAs during starvation in yeast. *Nature* **514**, 117–121 (2014).
17. Zipor, G. *et al.* Localization of mRNAs coding for peroxisomal proteins in the yeast, *Saccharomyces cerevisiae*. *Proc. Natl. Acad. Sci. USA* **106**, 19848–19853 (2009).
18. Long, R.M. *et al.* Mating type switching in yeast controlled by asymmetric localization of *ASH1* mRNA. *Science* **277**, 383–387 (1997).
19. Zenklusen, D., Larson, D.R. & Singer, R.H. Single-RNA counting reveals alternative modes of gene expression in yeast. *Nat. Struct. Mol. Biol.* **15**, 1263–1271 (2008).
20. Hocine, S., Raymond, P., Zenklusen, D., Chao, J.A. & Singer, R.H. Single-molecule analysis of gene expression using two-color RNA labeling in live yeast. *Nat. Methods* **10**, 119–121 (2013).
21. Wu, B. *et al.* Synonymous modification results in high-fidelity gene expression of repetitive protein and nucleotide sequences. *Genes Dev.* **29**, 876–886 (2015).
22. Mueller, F. *et al.* FISH-quant: automatic counting of transcripts in 3D FISH images. *Nat. Methods* **10**, 277–278 (2013).
23. Lowary, P.T. & Uhlenbeck, O.C. An RNA mutation that increases the affinity of an RNA–protein interaction. *Nucleic Acids Res.* **15**, 10483–10493 (1987).
24. Valegård, K. *et al.* The three-dimensional structures of two complexes between recombinant MS2 capsids and RNA operator fragments reveal sequence-specific protein-RNA interactions. *J. Mol. Biol.* **270**, 724–738 (1997).
25. Lohr, D., Venkov, P. & Zlatanova, J. Transcriptional regulation in the yeast GAL gene family: a complex genetic network. *FASEB J.* **9**, 777–787 (1995).
26. Hsu, C. *et al.* Stochastic signalling rewires the interaction map of a multiple feedback network during yeast evolution. *Nat. Commun.* **3**, 682 (2012).
27. Simpson, C.E., Lui, J., Kershaw, C.J., Sims, P.F. & Ashe, M.P. mRNA localization to P-bodies in yeast is bi-phasic with many mRNAs captured in a late Bfr1p-dependent wave. *J. Cell Sci.* **127**, 1254–1262 (2014).
28. Haim-Vilmovsky, L. & Gerst, J.E. m-TAG: a PCR-based genomic integration method to visualize the localization of specific endogenous mRNAs *in vivo* in yeast. *Nat. Protoc.* **4**, 1274–1284 (2009).
29. Haimovich, G. *et al.* Gene expression is circular: factors for mRNA degradation also foster mRNA synthesis. *Cell* **153**, 1000–1011 (2013).
30. Kshirsagar, M. & Parker, R. Identification of Edc3p as an enhancer of mRNA decapping in *Saccharomyces cerevisiae*. *Genetics* **166**, 729–739 (2004).
31. Trcek, T., Larson, D.R., Moldón, A., Query, C.C. & Singer, R.H. Single-molecule mRNA decay measurements reveal promoter- regulated mRNA stability in yeast. *Cell* **147**, 1484–1497 (2011).
32. Long, R.M. *et al.* Characterization of transport and localization of *ASH1* mRNA in yeast. *Mol. Biol. Cell* **8**, 2060–2060 (1997).
33. Heym, R.G. & Niessing, D. Principles of mRNA transport in yeast. *Cell. Mol. Life Sci.* **69**, 1843–1853 (2012).
34. Pereira, G. & Schiebel, E. The role of the yeast spindle pole body and the mammalian centrosome in regulating late mitotic events. *Curr. Opin. Cell Biol.* **13**, 762–769 (2001).
35. Eser, P. *et al.* Periodic mRNA synthesis and degradation co-operate during cell cycle gene expression. *Mol. Syst. Biol.* **10**, 717 (2014).
36. Lionnet, T. *et al.* A transgenic mouse for *in vivo* detection of endogenous labeled mRNA. *Nat. Methods* **8**, 165–170 (2011).
37. Dolgosheina, E.V. *et al.* RNA mango aptamer-fluorophore: a bright, high-affinity complex for RNA labeling and tracking. *ACS Chem. Biol.* **9**, 2412–2420 (2014).
38. Guet, D. *et al.* Combining Spinach-tagged RNA and gene localization to image gene expression in live yeast. *Nat. Commun.* **6**, 8882 (2015).
39. Nelles, D.A. *et al.* Programmable RNA tracking in live cells with CRISPR/Cas9. *Cell* **165**, 488–496 (2016).
40. Aizer, A. *et al.* Quantifying mRNA targeting to P-bodies in living human cells reveals their dual role in mRNA decay and storage. *J. Cell Sci.* **127**, 4443–4456 (2014).
41. Chao, J.A., Patskovsky, Y., Almo, S.C. & Singer, R.H. Structural basis for the coevolution of a viral RNA–protein complex. *Nat. Struct. Mol. Biol.* **15**, 103–105 (2008).
42. Daigle, N. & Ellenberg, J. LambdaN-GFP: an RNA reporter system for live-cell imaging. *Nat. Methods* **4**, 633–636 (2007).
43. Brodsky, A.S. & Silver, P.A. Pre-mRNA processing factors are required for nuclear export. *RNA* **6**, 1737–1749 (2000).

ONLINE METHODS

Yeast cultures. All strains described are derived either by the *S. cerevisiae* background BY4741 (MATa; his3Δ1; leu2Δ0; met15Δ0; ura3Δ0) or W303 BMA64-1B (MATα ; ura3-1; trp1Δ 2; leu2-3,112; his3-11,15; ade2-1; can1-100), see **Supplementary Table 4**. Yeast cultures were exponentially grown in synthetic medium with 2% glucose. Cells were grown at 25 °C using constant shaking at 210 r.p.m. For each application (smFISH and live imaging), details of cell cultures are described in "Method details."

Mammalian cultures. Human U2OS osteoscarcoma cell line (American Type Culture Collection HTB-96) stable expressing tdMCP-GFP[6] was used to test the applicability of the MBSV6 system in mammalian cells. U2Os were grown at 37 °C and 5% CO2 in DMEM supplemented with 10% FBS, 4.5 g/L glucose and 1% penicillin–streptomycin. Cells were transiently transfected with SINAPsV5 (ref. 6) or SINAPsV6 (**Supplementary Table 4**) with lipofectamine 3000 24 h before being subjected to live imaging experiments. The U2OS cell line was originally purchased from ATCC. We regularly genotype our human cell lines to confirm that our cell lines match the ATCC database. This validation is done by the genomics facility at Albert Einstein College of Medicine. Cells were free of mycoplasma.

Bacteria cultures. MBP-MCP-His (pET336) was transformed into Rosetta2 cells (EMD Millipore). Cells were grown at 37 °C in LB (with ampicillin and chloramphenicol) until OD600 of 0.6. Protein expression was then induced with 1 mM IPTG for 4 h. Cell pellets were centrifuged and stored at −80 °C until ready for lysis. Lysis was performed by sonication in lysis buffer (50 mM Tris pH 7.2, 1.5 M NaCl, 1 mM EDTA, 1 mM DTT supplemented with one Complete EDTA-free protease inhibitor tablet (Roche)). After centrifugation of cell debris, the soluble protein was first purified by amylose-affinity chromatography (New England BioLabs) and subsequently by TALON affinity chromatography (Takara Bioscience). Protein concentration was measured using the absorbance at 280 nm and a computationally predicted extinction coefficient (ProtParam).

Method details. *Construction of yeast strains.* Yeast strains were constructed in the BY4741 or BMA64-1A background (**Supplementary Table 4**). All strains where a gene of interest was tagged with MBSs in the 3′ UTR, right after the STOP codon, were prepared as follow: PCR amplification of the MBS insert (see plasmids in **Supplementary Table 4**) followed by the kanamycin-resistance gene, flanked by Loxp sequences, was performed with oligos (see **Supplementary Table 4**) containing homology sequences (50–70 nt) for the specific gene. For all strains, the Kanamycin-resistance gene was removed by expressing the CRE recombinase under the control of the *GAL1* promoter (**Supplementary Table 4**). Genomic DNA was extracted using standard techniques, and PCR amplification of the 3′ UTR was loaded on a gel and sent for sequencing to verify the size of the insert.

Plasmid construction. The new MBS sequences, U or C-variants, 12×MBSV6 and 12xMBSV7 were synthetized by Genescript. To obtain the 24xMBSV6 and 24xMBSV7, we cloned the 12xMBS V6/V7 in tandem by using restriction enzymes BamHI and BglII. Orientation of the insert was confirmed by sequencing. The 12xMBS or 24xMBS variants were then subcloned in a pUC vector containing the Kanamycin-resistance gene flanked by Loxp sites by using the restriction enzymes BamHI SalI. The plasmid pET296 (CYC1p-MCP-NLS-2xGFP) was generated by inserting the *CYC1*p, amplified from genomic DNA of BY4741, with flanking restriction enzymes XhoI and BamHI. The NLS from SV40 was added at the C terminus of the MCP coding sequence by PCR amplification using a reverse oligo containing the NLS sequence, flanked by restriction enzymes BamHI and AgeI. The addition of a nuclear localization signal to the MCP reduced the cytoplasmic background during live imaging. In the SINAPsV5 plasmid the sequence of 24xMBSV5 was replaced by digesting with AgeI and ClaI restriction enzymes and inserting within the same site 24xMBSV6 amplified by PCR. For EMSAs a C-terminal His Tag was added by PCR, and MCP-His was cloned using BamHI and HindIII sites into a pMalc derivative that contains a Tobacco Etch Virus (TEV) site after the maltose-binding protein (plasmid pET336, **Supplementary Table 4**).

smFISH probes preparation. ASH1, DOA1, GAL1, MDN1, MBSV5, MBSV6, MBSV7 probes were designed using the StellarisTM Probe Designer by LGC Biosearch Technologies and purchased from Biosearch Technologies. *HSP104* and MBSORF probes were synthetized by Invitrogen-Thermo Fisher and labeled in the lab using Cy3 dyes (Amersham) as previously described[31]. Sequence and fluorophores for all the probes are provided in **Supplementary Table 4**.

Single-molecule FISH and image acquisition and analysis. Single-molecule FISH (smFISH) was performed as follows. Yeast strains were grown overnight at 25 °C in selective medium with 2% glucose. In the morning cells were diluted to OD600 0.1 and allowed to grow until OD600 0.3–0.4. Yeast strains tagged in the *GAL1* gene were grown for 24 h in SC-Leu supplemented with 2% Raffinose. At OD = 0.3, *GAL1* expression was induced with 0.2% galactose for 30 min, and decay was induced by adding 4% glucose, as described in **Figure 5a**. Cells were fixed by adding paraformaldehyde (32% solution, EM grade; Electron Microscopy Science #15714) to a final concentration of 4% and gently shaken at room temperature for 45 min. Cells were then washed three times with buffer B (1.2 M sorbitol and 100 mM potassium phosphate buffer pH = 7.5) and resuspended in 500 µL of spheroplast buffer (buffer B containing 20 mM VRC (Ribonucleoside–vanadyl complex NEB #S1402S), and 25 U of Lyticase enzyme (Sigma #L2524) per OD of cells for about 10 min at 30 °C. Digested cells were washed once with buffer B and resuspended in 1 mL of buffer B. 150 µL of cells were seeded on 18 mm polylysine-treated coverslips and incubated at 4 °C for 30 min. Coverslips were washed once with buffer B, gently covered with ice-cold 70% ethanol and stored at −20 °C. For hybridization, coverslips were rehydrated by adding 2× SSC at room temperature twice for 5 min. Coverslips were prehybridized with a mix containing 10% formamide (ACROS organics #205821000)/2× SSC, at room temperature for 30 min. For each coverslip the probe mix (to obtain a final concentration in the hybridization mix of 125 nM) was added to 5 µL of 10 mg/µL *E. coli* tRNA: ssDNA (1:1) mix and dried with a speed vac. The dried mix was resuspended in 25 µL of hybridization mix (10% formamide, 2× SSC, 1 mg/ml BSA, 10 mM VRC, 5 mM NaHPO4 pH 7.5) and heated at 95 °C for 3 min. Cells were then hybridized at 37 °C for 3 h in the dark. Upon hybridization, coverslips were washed twice with prehybridization mix for 30 min at 37 °C, once with 0.1% Triton X-100 in 2× SSC

doi:10.1038/nmeth.4502

for 10 min at room temperature and once with 1× SSC for 10 min at room temperature. Nuclei were stained with 0.5 μg/mL DAPI in 1× PBS for 2 min at room temperature, washed with 1× PBS for 10 min at room temperature. Coverslips were mounted on glass slides using ProLong Gold antifade (Thermo Fisher). Images were acquired using an Olympus BX61 wide-field epifluorescence microscope with a 100×/1.35 NA UPlanApo objective. Samples were visualized using an X-Cite 120 PC lamp (EXFO) and the ORCA-R2 Digital CCD camera (Hamamatsu). Metamorph software (Molecular Devices) was used for acquisition. *Z*-sections were acquired at 200 nm intervals over an optical range of 8.0 μm. Image pixel size: *XY*, 64.5 nm. FISH images were analyzed using FISHQUANT[22]. Briefly, after background subtraction, the FISH spots in the cytoplasm were fit to a three-dimensional (3D) Gaussian to determine the coordinates of the mRNAs. The intensity and width of the 3D Gaussian were thresholded to exclude nonspecific signal. The average intensity of all the mRNAs was used to determine the intensity of each transcription site.

Sample preparation for live yeast fluorescence imaging. Yeast cells were grown at 25 °C in synthetic selective medium. Exponentially growing cells (O.D. 0.2–0.4) were plated on coated Delta-T dishes (Bioptech- 04200417C). The dishes were coated by incubation with Concanavalin A 1 mg/ml (Cayman chemical company) for 10 min at room temperature. Excess liquid was aspirated and dishes were dried at room temperature. To activate Concanavalin A, dishes were incubated for 10 min at room temperature with a 50 mM $CaCl_2$, 50 mM $MnCl_2$ solution. Excess was removed, and dishes were dried at room temperature. Finally, dishes were washed once with ultrapure water (Invitrogen) and let completely dry at room temperature. Cells attachment was performed by gravity for 20 min at room temperature, and excess liquid was removed and substituted with fresh media.

Glucose deprivation was performed by growing cells cotransformed with plasmids MCP-2× GFP and Edc3-mCherry in double-selective medium with 2% glucose overnight at 25 °C. Cells were diluted in the morning and grown until OD600 0.3–0.4. Cells were plated on dishes coated with Concanavalin A. Images were acquired before glucose starvation; then, keeping the dishes on the microscope stage with appropriate temperature control, washes were performed six times with 1 ml of medium without glucose. Cells were then kept in medium lacking glucose at 25 °C, and *z*-stacks were taken every minute for 40 min.

Live-cell fluorescence imaging and image analysis. The two-color simultaneous imaging of mRNAs and the appropriate cellular marker were performed on a modified version of the home-built microscope described in[6]. Briefly, the microscope was built around an IX71 stand (Olympus). For excitation, a 491 nm laser (CalypsoTM, Cobolt) and a 561 nm laser (JiveTM, Cobolt) were combined and controlled by an acoustic-optic tunable filter (AOTF, AOTFnC-400.650-TN, AA Opto-electronic) before being coupled into a single-mode optical fiber (Qioptiq). The output of the fiber was collimated and delivered through the back port of the microscope and reflected into an Olympus 150× 1.45 NA oil-immersion objective lens with a dichroic mirror (zt405/488/561rpc, 2 mm substrate, Chroma). The tube lens (180 mm focal length) was removed from the microscope and placed outside of the right port. A triple-band notch-emission filter (zet405/488/561m) was used to filter the scattered laser light. A dichroic mirror (T560LPXR, 3 mm substrate, Chroma) was used to split the fluorescence onto two precisely aligned EMCCDs (Andor iXon3, Model DU897) mounted on alignment stages (x, y, z, θ and φ angle). Emission filters FF03-525/50-25 and FF01-607/70-25 (Semrock) were placed in front of green and red channel cameras, respectively. The two cameras were triggered for exposure with a TTL pulse generated on a DAQ board (Measurement Computing). The microscope was equipped with a piezo stage (ASI) for fast *z*-stack and a Delta-T incubation system (Bioptech) for live-cell imaging. The microscope (AOTF, DAQ, Stage and Cameras) was automated with the software Metamorph (Molecular Devices). For two-color live-cell imaging, yeast cells were streamed at 50 ms, *Z* plane was streamed, and *Z*-stacks were acquired every 0.5 μm. Single-molecule analysis was done on the *Z*-stacked maximum projected images using AIRLOCALIZE[36].

Recombinant protein preparation. Transformation of pET336 and purification were performed as previously described[41]. In brief, constructs were transformed into Rosetta2 cells (EMD Millipore), and protein induction was performed for 4 h at 37 °C. Cell pellets were lysed by sonication in 50 mM Tris pH 7.2, 1.5 M NaCl, 1 mM EDTA, 1 mM DTT supplemented with one Complete EDTA-free protease inhibitor tablet (Roche). After centrifugation, the soluble protein was first purified by amylase-affinity chromatography (New England BioLabs) and subsequently by TALON-affinity chromatography (Takara Bioscience).

Electrophoretic mobility shift assay. Single stem–loop fragments with 5′ fluorescein modification (Dharmacon) were deprotected as per manufacturer recommendation. Prior to the experiment, RNA stocks were heated to 70 °C for 5 min then snap cooled on ice. The sequences of the RNAs used for these experiments are listed in **Supplementary Table 4**. Complexes were monitored and quantified by electrophoretic mobility shift assay (EMSA) as previously described[41]. In brief, 100 pM RNAs were incubated at room temperature for 3 h with two-fold dilutions of MCP in 10 mM Tris, 100 mM NaCl, 0.1 mM EDTA, 0.01 mg/mL tRNA, 50 μg/mL heparin and 0.01% IGEPAL CA630. Complexes were then run using 5% native PAGE in 0.5× TBE and visualized using the Typhoon 9400 variable mode laser scanner (GE Healthcare). Uncropped gels are shown in **Supplementary Figure 11**.

RNA preparation and northern blots. Total mRNA was isolated from yeast cultures grown at 25 °C in synthetic selective medium as described in refs. 11,13. For strains tagged in the *GAL1* gene, yeast were cultured overnight in 2% raffinose and then induced for 5 h with 0.2% galactose. Northern blots were performed by resolving 10 μg total RNA on 1.5% formaldehyde agarose gel, transferring by capillary action to a Nytran membrane and probing blots with [^{32}P] end-labeled oligonucleotide complementary to the 3′ UTR of *ASH1* (5′-ACAAGGAGAGAAATGTACAATTGTTTCG TGATAATGTCTCTTATTAGTTG-3′) and *GAL1* (5′-AAATGA GAAGTTGTTCTGAAACAAAGTAAA-3′ and 5′-TTGCGTAT TTGTGATGCTAAAGTTATGAGTAGA-3′) as described in refs. 11,13. Blots were stripped and reprobed for the 7S RNA using the following probe oRP100 (5′–GTCTAGCCGCGAGGAAGG–3′). Blots were visualized using a phosphoimager. Original northern blots are shown in **Supplementary Figure 12**.

Quantification and statistical analysis. FISH-quant was used to quantify single mRNA molecules in fixed samples[22]. Airlocalize

was used to quantify single mRNA molecules in live cells[36]. GraphPad Prism was used to calculate the mean and the s.d. of all the data and to perform the statistical analysis. The distribution of the mRNAs as reported in all 'frequency distribution plots' was generated using the same binning. For each experiment the *n*, statistical analysis applied and significance ($P < 0.05$ for significant differences) is indicated in the figure legend or the results section of the main text. All cells that fulfill the requirements for single-molecule detection were included in the analysis.

Life Sciences Reporting Summary. Further information on experimental design and reagents is available in the **Life Sciences Reporting Summary**.

Data availability statement. Further information and requests for resources and reagents should be directed to and will be fulfilled by the lead contact, R.H.S. (robert.singer@einstein.yu.edu). Plasmids are available at Addgene, accession numbers: 104390, 104391, 104392, 104393 and 104394.

doi:10.1038/nmeth.4502

nature research

Corresponding author(s): Robert H.Singer

☐ Initial submission ☒ Revised version ☐ Final submission

Life Sciences Reporting Summary

Nature Research wishes to improve the reproducibility of the work that we publish. This form is intended for publication with all accepted life science papers and provides structure for consistency and transparency in reporting. Every life science submission will use this form; some list items might not apply to an individual manuscript, but all fields must be completed for clarity.

For further information on the points included in this form, see Reporting Life Sciences Research. For further information on Nature Research policies, including our data availability policy, see Authors & Referees and the Editorial Policy Checklist.

Experimental design

1. Sample size

Describe how sample size was determined.

Base on previously published literature.

2. Data exclusions

Describe any data exclusions.

Cells with MBS aggregates were excluded from the anlysis of single mRNA counting. The strong brightness of the aggregated did not allow the quantification of single mRNAs. This is detailed in the text.

3. Replication

Describe whether the experimental findings were reliably reproduced.

All experiments were replicated at least two times. The results are reported as avergae of multiple experiments with hteir varaiance.

4. Randomization

Describe how samples/organisms/participants were allocated into experimental groups.

Does not apply

5. Blinding

Describe whether the investigators were blinded to group allocation during data collection and/or analysis.

Does not apply

Note: all studies involving animals and/or human research participants must disclose whether blinding and randomization were used.

6. Statistical parameters

For all figures and tables that use statistical methods, confirm that the following items are present in relevant figure legends (or in the Methods section if additional space is needed).

n/a	Confirmed	
☐	☒	The exact sample size (*n*) for each experimental group/condition, given as a discrete number and unit of measurement (animals, litters, cultures, etc.)
☐	☒	A description of how samples were collected, noting whether measurements were taken from distinct samples or whether the same sample was measured repeatedly
☐	☒	A statement indicating how many times each experiment was replicated
☐	☒	The statistical test(s) used and whether they are one- or two-sided (note: only common tests should be described solely by name; more complex techniques should be described in the Methods section)
☒	☐	A description of any assumptions or corrections, such as an adjustment for multiple comparisons
☐	☒	The test results (e.g. *P* values) given as exact values whenever possible and with confidence intervals noted
☐	☒	A clear description of statistics including central tendency (e.g. median, mean) and variation (e.g. standard deviation, interquartile range)
☐	☒	Clearly defined error bars

See the web collection on statistics for biologists for further resources and guidance.

Nature Methods: doi:10.1038/nmeth.4502

Software

Policy information about availability of computer code

7. Software

Describe the software used to analyze the data in this study.	1: Previously bublished software to quantify single mRNA molecules in fixed (Mueller et al.) or live cells (Lionnet et al.) 2: Matlab script to design the new MS2 arrays. This software is available upon request.

For manuscripts utilizing custom algorithms or software that are central to the paper but not yet described in the published literature, software must be made available to editors and reviewers upon request. We strongly encourage code deposition in a community repository (e.g. GitHub). *Nature Methods* guidance for providing algorithms and software for publication provides further information on this topic.

Materials and reagents

Policy information about availability of materials

8. Materials availability

Indicate whether there are restrictions on availability of unique materials or if these materials are only available for distribution by a for-profit company.	The material in this manuscript is the subject of a provisional application to the US Patent and Trademark Office. It has not been licensed to any corporation, and the authors (E.T, M.V. and R.H.S) are the sole inventors

9. Antibodies

Describe the antibodies used and how they were validated for use in the system under study (i.e. assay and species).	Does not apply.

10. Eukaryotic cell lines

a. State the source of each eukaryotic cell line used.	ATCC
b. Describe the method of cell line authentication used.	Genotyping through the Genomic Facility at the Albert Einstein College of Medicine.
c. Report whether the cell lines were tested for mycoplasma contamination.	Yes. No contamination detected.
d. If any of the cell lines used are listed in the database of commonly misidentified cell lines maintained by ICLAC, provide a scientific rationale for their use.	*Provide a rationale for the use of commonly misidentified cell lines OR state that no commonly misidentified cell lines were used.*

Animals and human research participants

Policy information about studies involving animals; when reporting animal research, follow the ARRIVE guidelines

11. Description of research animals

Provide details on animals and/or animal-derived materials used in the study.	*For laboratory animals, report species, strain, sex and age OR for animals observed in or captured from the field, report species, sex and age where possible OR state that no animals were used.*

Policy information about studies involving human research participants

12. Description of human research participants

Describe the covariate-relevant population characteristics of the human research participants.	*Provide all relevant information on human research participants, such as age, gender, genotypic information, past and current diagnosis and treatment categories, etc. OR state that the study did not involve human research participants.*

Nature Methods: doi:10.1038/nmeth.4502